# Digital spatial profiling of invasive lobular breast carcinoma

*San Antonio Breast Cancer Symposium - December 6-10, 2022*

Lynda B. Bennett[1,2], Sunati Sahoo[4], Cheryl M. Lewis[1,3], Indu Raman[1], Candace Frerich[1,2], Guanchun Chen[1], Min Xu[1] and Suzanne D. Conzen[1,2,3]

[1]UT Southwestern Medical Center, [2]Division of Hematology & Oncology, [3]Simmons Cancer Center, [4]Dept. of Pathology

UT Southwestern Medical Center

## Introduction

Invasive lobular breast cancer (ILC) is an understudied subtype of breast cancer with late recurrence, metastasis to serosal surfaces, such as the peritoneum, and dismal long-term outcome. The dynamic interaction between a tumor and its microenvironment (TME) leads to phenotypic changes in stromal cells and the extracellular matrix to promote growth or invasion of malignant cells. ILC is histologically distinct from invasive ductal carcinoma, characterized by discohesive tumor cells that grow as “single file” due to lack of the cell adhesion molecule E-cadherin. We therefore expect the TME to be quite unique in ILC. We hypothesized that differing levels of expression of nuclear receptors by tumor cells would impact cells residing within the stroma, presumably through paracrine signaling.

The nanoString GeoMx Digital Spatial Profiling (DSP) platform is a powerful tool to spatially resolve and quantify RNA and/or protein expression in archived or fresh tissue samples. Tissues can be optically segmented to profile tumor cells and tumor associated microenvironment (TME) separately. We performed DSP using segmentation into Pan-cytokeratin-positive (tumor) and negative sectors (TME) to interrogate differential gene and protein expression between GR-positive and GR-negative tumors in malignant cells and associated stromal regions in the tumor microenvironment (TME) of ILC in 12 invasive lobular breast cancer (ILC). We also utilized the spatial deconvolution tool to assess the contribution of tumor and immune cell-types in the tumor and TME in specimens with disparate expression of the glucorticoid receptor (GR). A comparison of GR high and GR low ILC tumors will lend insight into the proliferative and adhesive gene expression changes elicited by GR activation.

## Methods

The ILC FFPE tissue sections were stained with four morphology markers: Fluorescent antibody markers for DNA (SYTO13), Pan cytokeratin (Cy3), CD45 (Texas Red) (pseudo-colored yellow). For the RNA asays, a RNAscope probe for *NR3C1* (GR) tagged with Cy5. For the protein assays, a Cy5 labeled antibody was used.

Selection of regions of interest,(ROIs), segmentation for PanCK and statistical analyses were conducted within the GeoMx DSP Analysis Suite Version 2.4.0.421. Spatial deconvolution to obtain cell type abundances was performed using a plug-in tool from nanoString and the tumor/immune cell matrix (https://pubmed.ncbi.nlm.nih.gov/35046414/). Pathway analyses were performed using Gene Set Enrichment Ananlyses (GSEA)

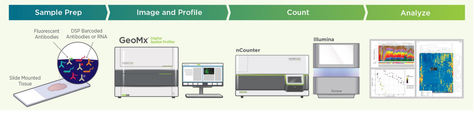


## Results

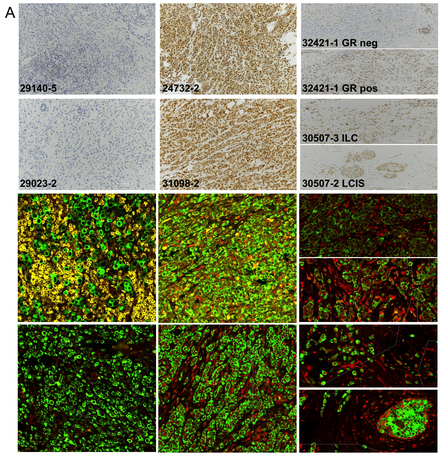


**Figure 1.** (A) Top: IHC for GR showing 2 cases positive for GR, two negative and two mixed (top). Bottom: Fluorescent images showing fluorescent antibody staining for morphology markers: PanCK (green), PanCK (yellow) and GR (red).(B) Segmentation for PanCK. ROIs are indicated by rectangles and numbers (Left). Right shows the mask for the stroma. From each ROI, RNA tags were collected for two AOIs, PanCK+ and PanCK- C) Unsupervised clustering for all cases. Each row is a gene; each column is an AOI. Color bars below heat map show PanCK+ and PanCK- AOIs and GR+ and GR- AOIs

## Results cont:

A

| Reactome pathway | Pathway description | Normalized enrichment score | pValue | Adjusted pValue |
|---|---|---|---|---|
| R-HSA-156842 | Eukaryotic Translation Elongation | 6.08 | 0.0002 | 0.00 |
| R-HSA-72764 | Eukaryotic Translation Termination | 6.07 | 0.0002 | 0.00 |
| R-HSA-156902 | Peptide chain elongation | 6.03 | 0.0002 | 0.00 |
| R-HSA-975956 | Nonsense Mediated Decay (NMD) independent of the Exon Junction Complex (EJC) | 6.03 | 0.0002 | 0.00 |
| R-HSA-192823 | Viral mRNA Translation | 6.02 | 0.0002 | 0.00 |
| R-HSA-156827 | L13a-mediated translational silencing of Ceruloplasmin expression | 6.00 | 0.0002 | 0.00 |
| R-HSA-72689 | Formation of a pool of free 40S subunits | 5.93 | 0.0002 | 0.00 |
| R-HSA-2408557 | Selenocysteine synthesis | 5.92 | 0.0002 | 0.00 |
| R-HSA-72706 | GTP hydrolysis and joining of the 60S ribosomal subunit | 5.91 | 0.0002 | 0.00 |
| R-HSA-72613 | Eukaryotic Translation Initiation | 5.89 | 0.0002 | 0.00 |
| R-HSA-72737 | Cap-dependent Translation Initiation | 5.89 | 0.0002 | 0.00 |
| R-HSA-9633012 | Response of EIF2AK4 (GCN2) to amino acid deficiency | 5.85 | 0.0002 | 0.00 |
| R-HSA-1799339 | SRP-dependent cotranslational protein targeting to membrane | 5.79 | 0.0002 | 0.00 |
| R-HSA-927802 | Nonsense-Mediated Decay (NMD) | 5.76 | 0.0002 | 0.00 |
| R-HSA-975957 | Nonsense Mediated Decay (NMD) enhanced by the Exon Junction Complex (EJC) | 5.76 | 0.0002 | 0.00 |
| R-HSA-2408522 | Selenoamino acid metabolism | 5.65 | 0.0002 | 0.00 |
| R-HSA-168273 | Influenza Viral RNA Transcription and Replication | 5.38 | 0.0002 | 0.00 |
| R-HSA-9010553 | Regulation of expression of SLITs and ROBOs | 5.35 | 0.0002 | 0.00 |
| R-HSA-168255 | Influenza Infection | 5.23 | 0.0002 | 0.00 |
| R-HSA-376176 | Signaling by ROBO receptors | 4.91 | 0.0002 | 0.00 |

| Reactome pathway ID | Pathway description | Normalized enrichment score | pValue | Adjusted pValue |
|---|---|---|---|---|
| R-HSA-909733 | Interferon alpha/beta signaling | -3.89373292 | 0.000197 | 0.004022 |
| R-HSA-877300 | Interferon gamma signaling | -3.58917407 | 0.000196 | 0.004022 |
| R-HSA-913531 | Interferon Signaling | -3.123562934 | 0.000196 | 0.004022 |
| R-HSA-1474290 | Collagen formation | -2.91125535 | 0.000197 | 0.004022 |
| R-HSA-198933 | Immunoregulatory interactions between a Lymphoid and a non-Lymphoid cell | -2.862962473 | 0.000199 | 0.004022 |
| R-HSA-983170 | Antigen Presentation: Folding, assembly and peptide loading of class I MHC | -2.822704839 | 0.000198 | 0.004022 |
| R-HSA-913709 | O-linked glycosylation of mucins | -2.781509018 | 0.000197 | 0.004022 |
| R-HSA-1650814 | Collagen biosynthesis and modifying enzymes | -2.758454027 | 0.000195 | 0.004022 |
| R-HSA-5173105 | O-linked glycosylation | -2.617924266 | 0.000199 | 0.004022 |
| R-HSA-2022090 | Assembly of collagen fibrils and other multimeric structures | -2.596838294 | 0.00009 | 0.007436 |
| R-HSA-1474244 | Extracellular matrix organization | -2.502956027 | 0.000195 | 0.004022 |
| R-HSA-196807 | Nicotinate metabolism | -2.464321496 | 0.0002 | 0.004022 |
| R-HSA-1442490 | Collagen degradation | -2.33230244 | 0.001377 | 0.022168 |
| R-HSA-8978868 | Fatty acid metabolism | -2.328033205 | 0.000589 | 0.010519 |
| R-HSA-8948216 | Collagen chain trimerization | -2.283128102 | 0.000599 | 0.010519 |
| R-HSA-196854 | Metabolism of vitamins and cofactors | -2.133339343 | 0.001777 | 0.026286 |
| R-HSA-2299718 | Condensation of Prophase Chromosomes | -2.12621108 | 0.003753 | 0.038101 |
| R-HSA-5625886 | Activated PKN1 stimulates transcription of AR (androgen receptor) regulated genes KLK2 and KLK | -2.093283643 | 0.003163 | 0.040509 |
| R-HSA-202733 | Cell surface interactions at the vascular wall | -2.091044766 | 0.002546 | 0.035811 |
| R-HSA-427359 | SIRT1 negatively regulates rRNA expression | -2.04421263 | 0.004928 | 0.05237 |

B

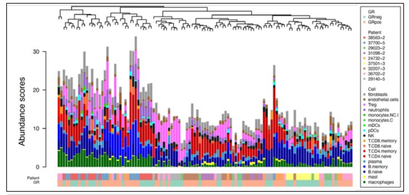


C

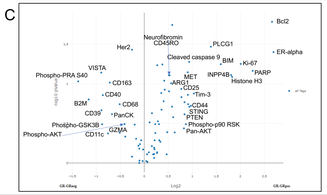


**Figure 2.** Linear mixed model (LMM) analyses were performed to test differential gene or protein expression between the tumors of 5 GR+ and 4 GR- ILC. (A) Gene expression GSEA pathways enriched in GR+ tumor cells (left) or GR- tumor cells (right). (B) Spatial deconvolution to measure the abundance of cell subsets based on RNA expression. Each bar represents one AOI. Color bars beneath graph is colored by patient and GR+/GR- (C) Volcano plot from LMM analysis of protein expression in GR+ vs GR- ILC

A

| Reactome pathway | Pathway description | Normalized enrichment score | pValue | Adjusted pValue |
|---|---|---|---|---|
| R-HSA-156827 | L13a-mediated translational silencing of Ceruloplasmin expression | 8.08 | 0.0002 | 0.002 |
| R-HSA-156842 | Eukaryotic Translation Elongation | 8.03 | 0.0002 | 0.002 |
| R-HSA-72706 | GTP hydrolysis and joining of the 60S ribosomal subunit | 7.99 | 0.0002 | 0.002 |
| R-HSA-72764 | Eukaryotic Translation Termination | 7.98 | 0.0002 | 0.002 |
| R-HSA-156902 | Peptide chain elongation | 7.97 | 0.0002 | 0.002 |
| R-HSA-72689 | Formation of a pool of free 40S subunits | 7.95 | 0.0002 | 0.002 |
| R-HSA-72613 | Eukaryotic Translation Initiation | 7.95 | 0.0002 | 0.002 |
| R-HSA-72737 | Cap-dependent Translation Initiation | 7.95 | 0.0002 | 0.002 |
| R-HSA-975956 | Nonsense Mediated Decay (NMD) independent of the Exon Junction Complex (EJC) | 7.92 | 0.0002 | 0.002 |
| R-HSA-192823 | Viral mRNA Translation | 7.89 | 0.0002 | 0.002 |
| R-HSA-2408557 | Selenocysteine synthesis | 7.87 | 0.0002 | 0.002 |
| R-HSA-9633012 | Response of EIF2AK4 (GCN2) to amino acid deficiency | 7.85 | 0.0002 | 0.002 |
| R-HSA-1799339 | SRP-dependent cotranslational protein targeting to membrane | 7.69 | 0.0002 | 0.002 |
| R-HSA-927802 | Nonsense-Mediated Decay (NMD) | 7.48 | 0.0002 | 0.002 |
| R-HSA-975957 | Nonsense Mediated Decay (NMD) enhanced by the Exon Junction Complex (EJC) | 7.48 | 0.0002 | 0.002 |
| R-HSA-2408522 | Selenoamino acid metabolism | 7.45 | 0.0002 | 0.002 |
| R-HSA-168255 | Influenza Infection | 7.22 | 0.0002 | 0.002 |
| R-HSA-9010553 | Regulation of expression of SLITs and ROBOs | 7.21 | 0.0002 | 0.002 |
| R-HSA-168273 | Influenza Viral RNA Transcription and Replication | 7.09 | 0.0002 | 0.002 |
| R-HSA-376176 | Signaling by ROBO receptors | 7.00 | 0.0002 | 0.002 |

| Reactome pathway | Pathway description | Normalized enrichment score | pValue | Adjusted pValue |
|---|---|---|---|---|
| R-HSA-1650814 | Collagen biosynthesis and modifying enzymes | -3.63 | 0.0002 | 0.002 |
| R-HSA-1474290 | Collagen formation | -3.48 | 0.0002 | 0.002 |
| R-HSA-5173105 | O-linked glycosylation | -3.28 | 0.0002 | 0.002 |
| R-HSA-1474244 | Extracellular matrix organization | -2.99 | 0.0002 | 0.002 |
| R-HSA-8948216 | Collagen chain trimerization | -2.78 | 0.0002 | 0.002 |
| R-HSA-2022090 | Assembly of collagen fibrils and other multimeric structures | -2.67 | 0.0002 | 0.002 |
| R-HSA-3906995 | Diseases associated with O-glycosylation of proteins | -2.65 | 0.0002 | 0.002 |
| R-HSA-913709 | O-linked glycosylation of mucins | -2.55 | 0.0002 | 0.002 |
| R-HSA-1442490 | Collagen degradation | -2.47 | 0.0008 | 0.003 |
| R-HSA-3781865 | Diseases of glycosylation | -2.47 | 0.0004 | 0.002 |
| R-HSA-5668914 | Diseases of metabolism | -2.34 | 0.0006 | 0.003 |
| R-HSA-1566948 | Elastic fibre formation | -2.21 | 0.0024 | 0.007 |
| R-HSA-216083 | Integrin cell surface interactions | -2.19 | 0.0018 | 0.006 |
| R-HSA-2129379 | Molecules associated with elastic fibres | -2.17 | 0.0036 | 0.011 |
| R-HSA-3000170 | Syndecan interactions | -2.16 | 0.0038 | 0.012 |
| R-HSA-198933 | Immunoregulatory interactions between a Lymphoid and a non-Lymphoid cell | -2.13 | 0.0016 | 0.006 |
| R-HSA-3000178 | ECM proteoglycans | -2.08 | 0.0030 | 0.010 |
| R-HSA-1474228 | Degradation of the extracellular matrix | -1.98 | 0.0055 | 0.016 |
| R-HSA-202733 | Cell surface interactions at the vascular wall | -1.97 | 0.0045 | 0.014 |
| R-HSA-3000171 | Non-integrin membrane-ECM interactions | -1.92 | 0.0094 | 0.025 |

B

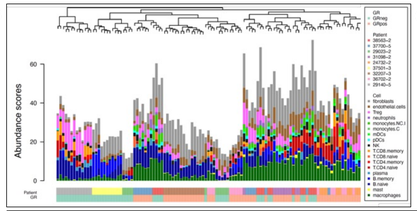


C

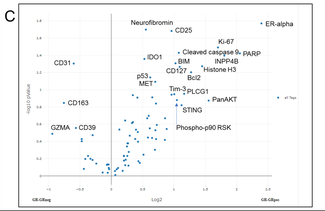


**Figure 3.** Linear mixed model (LMM) analyses were performed to test differential gene and protein expression between the TME of 5 GR+ and 4 GR- tumors. (A) Gene expression GSEA pathways enriched in TME of GR+ (left) or GR- ILC(right). (B) Spatial deconvolution to measure the abundance of cell subsets based on the RNA expression. Each bar represents one AOI. Color bar beneath graph is colored by patient and GR+/GR- (C) Volcano plot from LMM analysis of protein expression TME of GR+ vs GR- ILC

## Results cont.

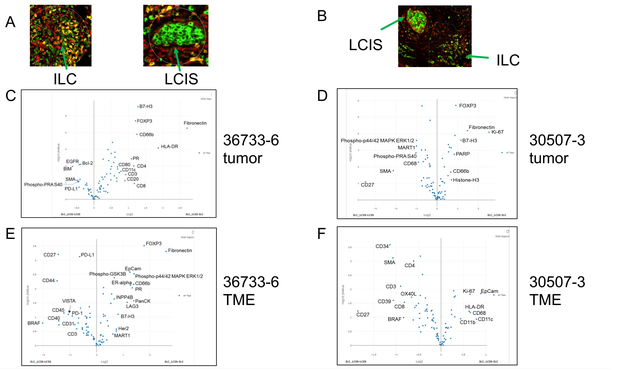


**Figure 4.** (A) Fluorescent images from protein DSP showing invasive ILC (left) and in situ LCIS (right) regions of the same tumor from case 36733-6 (GR-). (B) Fluorescent image from protein DSP showing ILC and LCIS regions of the same tumor from case 30507-3 (GR variable expression). (C-F) Volcano plots from LMM analysis of proteins differentially expressed between regions of invasive (ILC) vs in situ (LCIS) cancer. Analyses were performed separately for tumor or TME

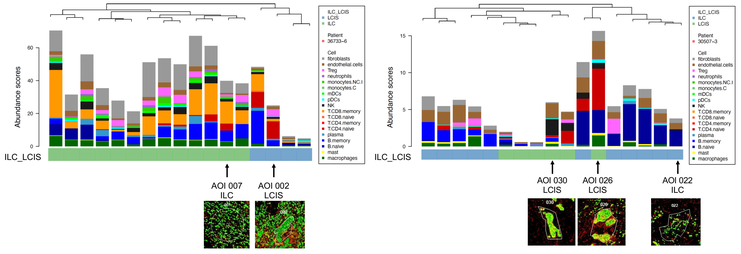


**Figure 5.** Abundance of tumor and immune cell types in the the TME represented by AOIs from ILC and LCIS regions of tumors from cases 36733-6 (left) and 30507-3 (right). Fluorescent images from selected AOIs are shown below the column that shows the abundance of the cell subsets. Tumor cells are labeled with Cy3 (green), CD45+ cells are labelled with Texas red (yellow) and *NR3C1* (GR) is labeled with C5 (red)

## Conclusions

- GR promotes an immune suppressive environment in ILC
- Patients’ ILC tumor microenvironment is heterogeneous regardless of GR expression in the tumor cells
- GR+ tumors may exclude cytotoxic T-cells
- Certain checkpoint proteins may be downregulated in GR expressing ILC
- GeoMx DSP is a powerful platform to resolve gene expression in a spatial context
- Reveals heterogeneity between and within tumors
- Gives insight into the localized variations in the complex milieu of the stroma
- Can analyze RNA and protein within the same ROIs